

MaskINT: Video Editing via Interpolative Non-autoregressive Masked Transformers

Haoyu Ma^{1*}, Shahin Mahdizadehaghdam², Bichen Wu², Zhipeng Fan², Yuchao Gu³,
Wenliang Zhao², Lior Shapira², Xiaohui Xie¹

¹University of California, Irvine, ²GenAI, Meta, ³National University of Singapore
<https://maskint.github.io>

Abstract

Recent advances in generative AI have significantly enhanced image and video editing, particularly in the context of text prompt control. State-of-the-art approaches predominantly rely on diffusion models to accomplish these tasks. However, the computational demands of diffusion-based methods are substantial, often necessitating large-scale paired datasets for training, and therefore challenging the deployment in practical applications. This study addresses this challenge by breaking down the text-based video editing process into two separate stages. In the first stage, we leverage an existing text-to-image diffusion model to simultaneously edit a few keyframes without additional fine-tuning. In the second stage, we introduce an efficient model called MaskINT, which is built on non-autoregressive masked generative transformers and specializes in frame interpolation between the keyframes, benefiting from structural guidance provided by intermediate frames. Our comprehensive set of experiments illustrates the efficacy and efficiency of MaskINT when compared to other diffusion-based methodologies. This research offers a practical solution for text-based video editing and showcases the potential of non-autoregressive masked generative transformers in this domain.

1. Introduction

Text-based video editing, which aims to modify a video’s content or style in accordance with a provided text description while preserving the motion and semantic layout, plays an important role in a wide range of applications, including advertisement, live streaming, and the movie industry, etc. This challenging task requires that edited video frames not only match the given text prompt but also ensure the consistency across all video frames.

Recently, numerous studies have showcased the impressive capabilities of diffusion models [18] in the domain of text-to-image and text-to-video generation [3, 37, 38, 40]. Later on, built upon Stable Diffusion (SD) [37], several works have achieved remarkable success in the realm of text-based image editing [4, 43, 52]. When extending to text-based video editing, existing works can be mainly divided into two ways: One is to train diffusion models with temporal modules on paired text-video datasets [13, 19]. However, due to the lack of extensive text-to-video datasets, these works typically struggle to achieve the same level of editing expertise seen in the realm of image editing. The other involves leveraging a pre-trained text-to-image diffusion models in a training-free techniques [15, 25, 34, 53]. These works usually extend the self-attention across all frames to achieve an overall temporal consistency. However, this attention-based temporal constraint remains implicit and suboptimal. Moreover, while diffusion-based techniques are capable of producing high-fidelity videos, the use of diffusion models to produce all video frames proves to be a highly time-consuming process. The integration of the global attention across all frames in these video editing methods further extends the processing time, rendering them less practical for real-world applications.

Meanwhile, studies indicate that non-autoregressive masked generative transformers [7, 8, 16, 51] can attain similar levels of performance in generating images or videos compared to diffusion-based methods, while bring significant efficiency [8]. These works first tokenize image or videos into a sequence of discrete tokens [12], and then train transformers [10, 44] with masked token modeling to predict these tokens. During the inference time, they employ non-autoregressive decoding, which generates all tokens in parallel and iteratively refine predictions in a few steps. Nonetheless, extending these techniques to perform global editing tasks, such as stylization, presents a formidable challenge. This type of task requires the replacement of nearly all tokens with new ones, as opposed to merely modifying tokens within a localized region.

*Work done during an internship at GenAI, Meta

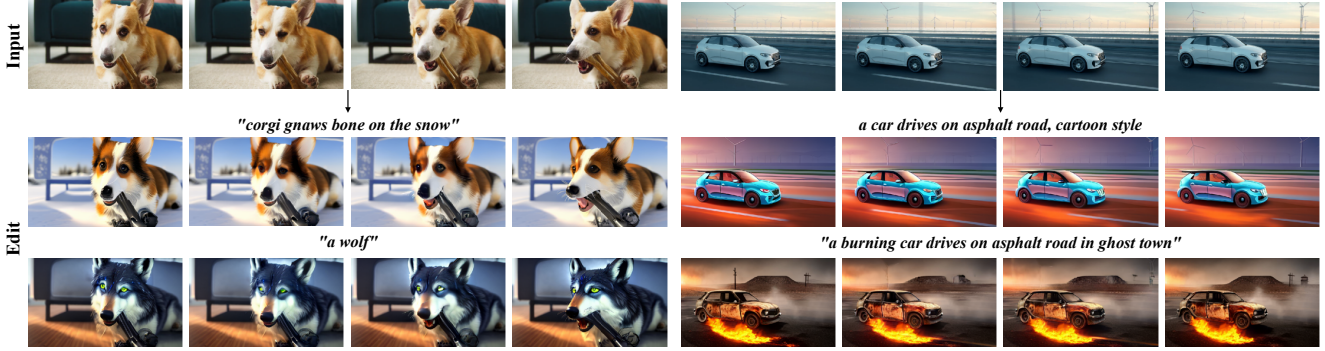


Figure 1. Examples of video editing with MaskINT.

In this paper, we disentangle text-based video editing into two separate stages. In the first stage, we utilize existing text-based image editing models to jointly edit only two keyframes (i.e., the initial and last frames) from the video, guided by the provided text prompt. In the second stage, we propose a novel Interpolative Non-autoregressive generative Transformers (MaskINT), which performs structure-aware frame interpolation by leveraging both the color information of the initial and final frames, as well as structural cues like edge or depth maps from intermediate frames. Through disentanglement of keyframe editing and frame interpolation into separate stages, our pipeline eliminates the requirement for paired video datasets during training, thereby enabling us to train the MaskINT using video-only datasets. Furthermore, thanks to its non-autoregressive decoding, MaskINT significantly accelerates the generation of intermediate frames compared to using diffusion models for this purpose. We show that our method balances the trade off between quality and efficiency, offering comparable performance with existing diffusion methods yet taking much less time in generation.

Our major contributions are summarized as follows:

- We propose to disentangle the text-based video editing into a two stage pipeline, that involves keyframes joint editing using existing image diffusion model and structure-aware frame interpolation with masked generative transformers trained on video only datasets.
- We propose MaskINT to perform structure-aware frame interpolation, which is the pioneer work that explicitly introduces structure control into non-autoregressive generative transformers.
- Experimental results demonstrate that our method achieves comparable performance with diffusion methods in terms of temporal consistency and alignment with text prompts, while providing 5-7 times faster inference times.

2. Related Work

Generative Transformers. Following GPT [5], many pioneer works [12, 14, 20, 26, 50] tokenize images/videos

into discrete tokens, and train *Autoregressive Generative Transformers* to perform image/video generation, where tokens are generated sequentially based on previous output. However, these autoregressive methods become exceedingly time-consuming when the length of the token sequence increases. Recently, *Non-autoregressive Generative Transformers*, capable of simultaneously generating all tokens in parallel, have emerged as efficient solutions [7, 51]. Specifically, MaskGiT [7] first shows the capability and efficiency of this technique in image generation. It can be seamlessly extended to tasks like inpainting and extrapolation by applying various initial mask constraints. Muse [8] achieves state-of-the-art performance in text-to-image generation by training on large-scale text-image datasets and brings significantly efficiency improvement. StyleDrop [41] further finetunes Muse with human feedback to perform text-to-image generation guided with a reference style image. Furthermore, MaskSketch [1] introduces implicit structural guidance into MaskGiT by calculating the similarity of attention maps in the sampling step. Nevertheless, this implicit structure condition is suboptimal.

In video generation, MaskViT [16] employ 2D tokenizer and trains a bidirectional window transformer to perform frame prediction. Phenaki [45] trains a masked transformer to generate short video clips condition on text prompt and extends it to arbitrary long video with different prompts in an autoregressive way. MAGViT [51] utilizes 3D tokenizer to quantize videos and trains a single model to perform multiple video generation tasks such as inpainting, outpainting, frame interpolation, etc. However, to the best of our knowledge, there is currently no existing literature in the field of text-based video editing utilizing masked generative transformers. Besides, there is a notable absence of research that delves into explicit structural control within this area.

Diffusion Models in Image Editing. Leveraging the advancements of SD [37], numerous studies have achieved significant success in the field of text-based image editing

[9, 17, 24, 29, 30, 32, 43, 52, 54]. For example, ControlNet [52], T2I-Adapter [30], and Composer [21] finetune SD with spatial condition such as depth maps and edge maps, enabling text-to-image synthesis with the same structure as the input image. The PNP [43] incorporates DDIM inversion features [42] from the input image into the text-to-image generation process alongside SD, enabling image editing without the necessity of additional training or finetuning. Instructpix2pix [4] trains a conditional diffusion model for text-guided image editing using synthetic paired examples, which avoid the tedious inversion. Nevertheless, employing these methods on each video frame independently often leads to inconsistencies and flickering.

Diffusion Models in Video Editing. Recently, diffusion models also dominate the field of video generation and video editing [19, 40]. For example, Gen-1 [13] trains a video diffusion models on paired text-video datasets to generate videos with both depth map and text prompts. Meanwhile, several works utilize pre-trained image diffusion models to achieve video editing in a training-free way [6, 25, 34, 46, 47, 49, 53]. To enable a cohesive global appearance among edited frames, a common approach in these studies involves extending the attention module of SD to encompass multiple frames and conducting cross-frame attention. In detail, Text2Video-Zero [25] performs cross-frame attention of each frame on the first frame to preserve appearance consistency. ControlVideo [53] extends ControlNet with fully cross-frame attention to joint edit all frames and further improves the performance with interleaved-frame smoother. TokenFlow [15] enhance PNP [43] with extended-attention to jointly edit a few keyframes at each denoising step and propagate them throughout the video based on nearest-neighbor field. On the contrary, we only utilize existing image diffusion models to edit two keyframes, rather than all video frames.

Video Frame Interpolation (VFI). VFI aims to generate intermediate images between a pair of frames, which can be applied to creating slow-motion videos and enhancing refresh rate. Advanced methods typically entail estimating dense motions between frames, like optical flow, and subsequently warping the provided frames to generate intermediate ones [22, 23, 28, 31, 36, 39]. However, these methods are most effective with simple or monotonous motion. Thus, they cannot be directly applied to the second stage. In our work, we perform frame interpolation by incorporating additional structural signals.

3. Preliminaries

3.1. Masked Generative Transformers

Masked generative transformers [7] follow a two-stage pipeline. In the first stage, an image is quantized into a sequence of discrete tokens via a Vector-Quantized (VQ)

auto-encoder [12]. In detail, given an image $\mathbf{I} \in \mathbb{R}^{H \times W \times 3}$, an encoder \mathcal{E} encodes it into a series of latent vectors and discretize them through a nearest neighbour look up in a codebook of quantized embeddings with size M . To this end, an image can be represented with a sequence of codebook’s indices $\mathbf{Z} = [z_i]_{i=1}^{h \times w}$, $z_i \in \{1, 2, \dots, M\}$, where h and w is the resolution of latent features. A decoder \mathcal{D} can reconstruct the indices back to image $\mathcal{D}(\mathbf{Z}) \approx \mathbf{I}$. In the second stage, a bidirectional transformer model [44] is learned with Masked Token Modeling (MTM). Specifically, during training, a random mask ratio $r \in (0, 1)$ is selected and $\lfloor \gamma(r) \cdot h \times w \rfloor$ tokens in Z are replaced with a special [MASK] token, where $\gamma(r)$ is a mask scheduling function [7]. We denote the corrupted sequence with masked tokens as $\bar{\mathbf{Z}}$ and conditions such as class labels or text prompt as \mathbf{c} . Given the training dataset \mathbb{D} , a BERT [10] parameterized by Φ is learned to minimize the cross-entropy loss between the predicted and the ground truth token at each masked position:

$$\mathcal{L}_{MTM} = \mathbb{E}_{\mathbf{z} \in \mathbb{D}} \left[\sum_{z_i = [\text{MASK}]} -\log p_{\Phi}(z_i | \bar{\mathbf{Z}}, \mathbf{c}) \right]. \quad (1)$$

During inference time, non-autoregressive decoding is applied to generate images. Specifically, given the conditions \mathbf{c} , all tokens are initialized as [MASK] tokens. At step k , all tokens are predicted in parallel while only tokens with the highest prediction scores are kept. The remaining tokens with least prediction scores are masked out and regenerated in the next iteration. The mask ratio is determined by $\gamma(\frac{k}{K})$ at step k , where K is the total number of iteration steps.

3.2. ControlNet

Latent Diffusion Models Denoising Diffusion Probabilistic Models (DDPM) [18] generate images through a progressive noise removal process applied to an initial Gaussian noisy image, carried out over a span of $T (>> K)$ time steps. To enable efficient high-resolution image generation, Latent Diffusion models [37] operates the diffusion process in the latent space of an autoencoder. First, an encoder \mathcal{E}' compresses an image \mathbf{I} to a low-resolution latent code $x = \mathcal{E}'(\mathbf{I}) \in \mathbb{R}^{h \times w \times c}$. Second, a U-Net ϵ_{θ} with attention modules [44] is trained to remove the noise with loss function:

$$\mathcal{L}_{LDM} = \mathbb{E}_{x_0, \epsilon \sim N(0, I), t \sim} \|\epsilon - \epsilon_{\theta}(x_t, t, \tau)\|_2^2, \quad (2)$$

where τ is the text prompt and x_t is the noisy latent sample at timestep t . Stable Diffusion is trained on datasets with billion scale text-image pairs, which serves as the foundation model of many generation tasks.

ControlNet In practice, it’s challenging to use text prompt to describe the layout of generated image. Furthermore, ControlNet [52] is proposed to provide spatial layout conditions such as edge map, depth map, and human

poses. In detail, ControlNet train the same U-Net architecture as SD and finetune it with specific conditions. We denote ControlNet as $\epsilon'_\theta(x_t, t, \tau, s)$, where s is the spatial layout condition.

4. Methodology

4.1. Overview

Fig. 2 shows an overview of our framework. We disentangle the video editing task into keyframe joint editing stage and structure-aware frame interpolation stage. Specifically, given a video clip with N frames $\{\mathbf{I}^i\}_{i=1}^N$, in the first stage, with the input text prompt τ , we simultaneously edit two keyframes, i.e., the initial frame \mathbf{I}^1 and last frame \mathbf{I}^N , using existing image-editing model $g(\cdot)$ that requires no additional tuning. This frame based joint editing module provides high-quality coherent edited frames $^*\mathbf{I}^1, ^*\mathbf{I}^N = g(\mathbf{I}^1, \mathbf{I}^N, \tau)$ and is highly efficient on a pair of frame. In the second stage, we propose MaskINT to perform structure-aware frame interpolation via non-autoregressive transformers. The entire edited video frames are generated by $\{^*\mathbf{I}^i\}_{i=1}^N = f_\Phi(^*\mathbf{I}^1, ^*\mathbf{I}^N, \{\mathbf{S}^i\}_{i=1}^N)$, where $\mathbf{S}^i \in [0, 1]^{H \times W \times 1}$ is the structural condition (i.e., the HED edge map [48]). Our MaskINT is trained with masked token modeling (MTM) on video only datasets, conditioning on the structural signal $\{\mathbf{S}^i\}_{i=1}^N$ as well as the initial frame \mathbf{I}^1 and last frame \mathbf{I}^N .

4.2. Keyframes Joint Editing

To maintain the structure layout of selected keyframes, we take ControlNet [52] to edit \mathbf{I}^1 and \mathbf{I}^N based on text prompt τ as well as their edge maps \mathbf{S}^1 and \mathbf{S}^N . However, even with the identical noise, applying ControlNet to each keyframes individually, i.e., $\epsilon'_\theta(x_t^1, t, \tau, \mathbf{S}^1)$ and $\epsilon'_\theta(x_t^N, t, \tau, \mathbf{S}^N)$, cannot guarantee the appearance consistency. To address this issue, following previous work [15, 47, 53], we extend the self-attention blocks to simultaneously process two keyframes. In detail, the self-attention block projects the noisy feature map x_t^j of j^{th} frame at time step t into query \mathbf{Q}^j , key \mathbf{K}^j , value \mathbf{V}^j in the original U-Net of SD. We extend the self-attention block to perform attention across all selected keyframes by concatenating their keys and values and calculate the attention by

$$\text{Softmax}\left(\frac{\mathbf{Q}^j[\mathbf{K}^1, \mathbf{K}^N]^T}{\sqrt{c}}\right)[\mathbf{V}^1, \mathbf{V}^N] \quad (3)$$

Note that although only two frames were used in Eq.3, this joint editing can seamlessly generalize to any number of frames, but at the cost of longer processing time and huge demand in resources.

4.3. MaskINT

Structural-aware embeddings. Previous works [16, 51] demonstrate that non-autoregressive masked generative transformers can effectively perform frame prediction and

interpolation tasks. However, these architectures lack explicit control of structure, making it difficult to follow the motion of original videos. In our work, we explicitly introduce structural condition of each frame into the generation process. Specifically, we tokenize both RGB frames $\{\mathbf{I}^i\}_{i=1}^N$ and structure maps $\{\mathbf{S}^i\}_{i=1}^N$ with an off-the-shelf 2D VQ tokenizer [12]. We utilize 2D VQ rather than 3D VQ [51] to accommodate varying numbers of frames and frame rate without constraints. We denote the tokens from RGB frames as $^c\mathbf{Z} = \{^cz_i\}_{i=1}^{N \times h \times w}$ (color token) and tokens from edge maps as $^s\mathbf{Z} = \{^sz_i\}_{i=1}^{N \times h \times w}$ (structure token), where $^sz_i, ^cz_i \in \{1, 2, \dots, M\}$, where M is the codebook size. Subsequently, two distinct embedding layers $e^C(\cdot)$ and $e^S(\cdot)$ are learned to map token indices $^c\mathbf{Z}$ and $^s\mathbf{Z}$ into their respective embedding spaces. Learnable 2D spatial positional encoding \mathbf{P}^S and temporal positional encoding \mathbf{P}^T are also added [2]. Thus, the input to the following transformer layers can be formulated by $\mathbf{X} = e^C(^c\mathbf{Z}) + e^S(^s\mathbf{Z}) + \mathbf{P}^S + \mathbf{P}^T \in \mathbb{R}^{N \times h \times w \times c}$.

Transformer with Window-Restricted Attention. Previous masked generative transformers [7, 51] employ a pure transformer with global attention [44]. However, Given that there is no substantial motion between consecutive frames, we adopt self-attention within a restricted window to further mitigate computational overhead, following MaskViT [16]. In detail, our approach involves two distinct stages of attention. Initially, we employ spatial window attention, confining attention to tokens within a frame of dimensions $1 \times h \times w$. Subsequently, we extend this to spatial-temporal window attention, which confines attention to tokens within a tube of dimensions $N \times h_w \times w_w$, where h_w and w_w is the window size, where $h_w < h$ and $w_w < w$, which greatly reduce the complexity. Besides, to further reduce computation of transformer, we also add a shallow convolution layers to downsample \mathbf{X} before the transformer encoder layers and an upsample layer at the end.

Training. By fully disentangling keyframes editing and frame interpolation into distinct stages, our model no longer necessitates paired videos for training. Consequently, we can train MaskINT using video only datasets. Denote the color token of i^{th} RGB frame as $^c\mathbf{Z}^i = \{^cz_i^i\}_{i=1}^{h \times w}$. During the training time, we keep color tokens of the initial frame $^c\mathbf{Z}^1$ and last frame $^c\mathbf{Z}^N$, and randomly replace $[\gamma(r) \cdot (N - 2) \cdot N]$ color tokens of intermediate frames with the [MASK] tokens. We denote this corrupted video color tokens as $^c\bar{\mathbf{Z}} = \{^c\mathbf{Z}^1, ^c\bar{\mathbf{Z}}^2, \dots, ^c\bar{\mathbf{Z}}^{N-1}, ^c\mathbf{Z}^N\}$. The structure-aware window-restricted transformer with parameters Θ is trained by

$$\mathcal{L}_{MTM} = \mathbb{E}_{^c\mathbf{Z}, ^s\mathbf{Z} \in \mathbb{D}} \left[\sum_{^cz_i = [\text{MASK}]} -\log p_\Theta(^cz_i | ^c\bar{\mathbf{Z}}, ^s\mathbf{Z}) \right] \quad (4)$$

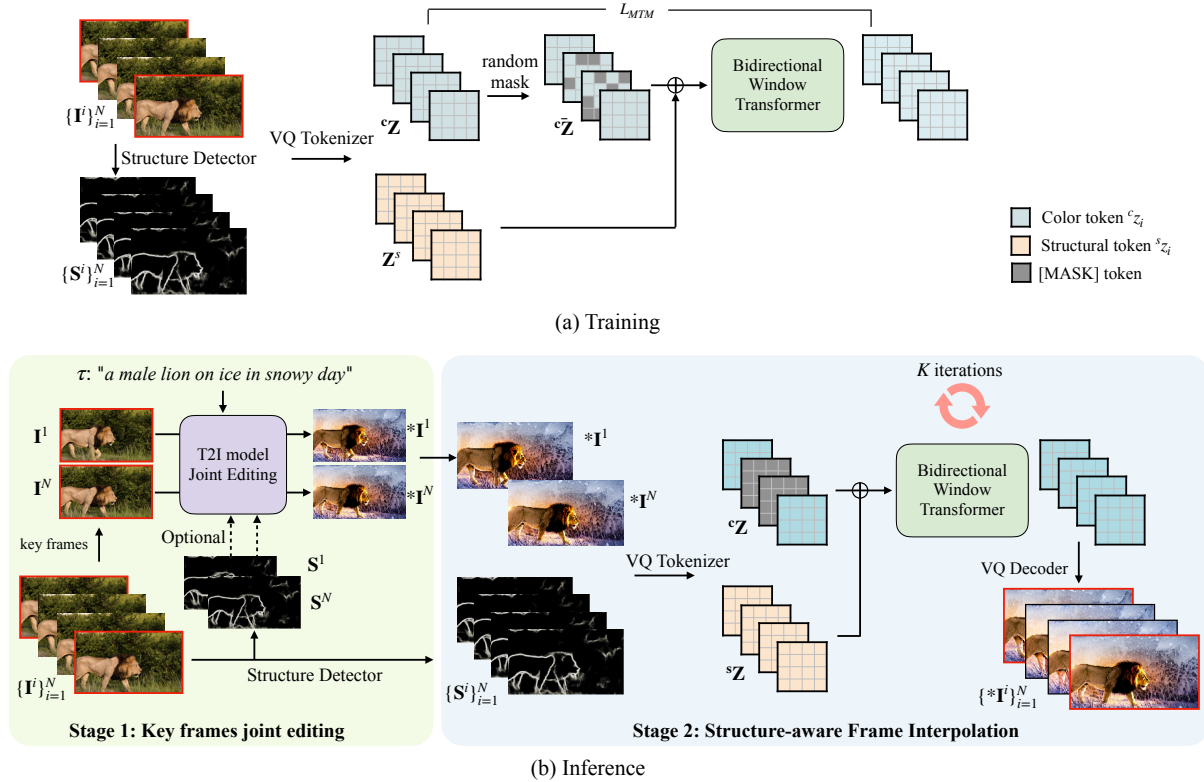


Figure 2. Overview of MaskINT. MaskINT disentangle the video editing task into two separate stages, i.e., keyframes joint editing and structure-aware frame interpolation.

Inference. During the inference time, our MaskINT can seamlessly generalize to perform frame interpolation between the jointly edited frames, although it is only trained with regular videos. Specifically, we tokenize the the initial and last edited frames $*\mathbf{I}^1$ and $*\mathbf{I}^N$ from Stage 1 into color tokens $*c^z_1$ and $*c^z_N$, and initialize color tokens of all intermediate frames $\{c^z_2, \dots, c^z_{N-1}\}$ with [MASK] tokens. We follow the iterative decoding in MaskGiT [7] with a total number of K steps. At step k , we predict all color tokens in parallel and keep tokens with the highest confidence score.

5. Experiments

5.1. Settings

Implementation Details. We train our model with 100k videos from Shutterstock website¹. During training time, we random select a $T = 16$ video clip with frame interval 1, 2, 4 from each video and resize it to 384×672 . We utilize Retina-VQ [11] with 8 downsample ratio, i.e., each frame has 48×84 tokens. We employ Transformer-Base as our MaskINT and optimized it from scratch with the AdamW optimizer [27] for a duration of 100 epochs. The initial learning rate is set to $1e-4$ and decayed with cosine schedule. During the inference time, we set the number of decod-

¹<https://www.shutterstock.com/video>

ing step K to 32 and the temperature t to 4.5.

Evaluation. Following [47], we use the selected 40 object-centric videos of the DAVIS dataset [33], covering humans, animals, vehicles, etc. Besides, we also select 30 unseen videos from the Shutterstock dataset. For each video, we manually design 5 edited prompts, including object editing, background changes and style transfers. Following previous works [34, 53], we assess the quality of the generated videos using CLIP [35]. In detail, we evaluate 1) Temporal consistency, which calculates the average cosine similarity of all pairs of consecutive frames. 2) Prompt consistency, which calculates the average cosine similarity between given text prompt and all video frames. To evaluate the efficiency, we report the duration required for generating a 16-frame video clip on a single NVIDIA A6000 GPU.

5.2. Results

We select methods that built upon text-to-image diffusion models for comparison, including TokenFlow [15], Text-to-video zero [25], and ControlVideo [53]. We also consider apply ControlNet to each frame individually with the same initial noise as baseline. Besides, we also compare with frame interpolation with FILM [36] with the same edited keyframes.

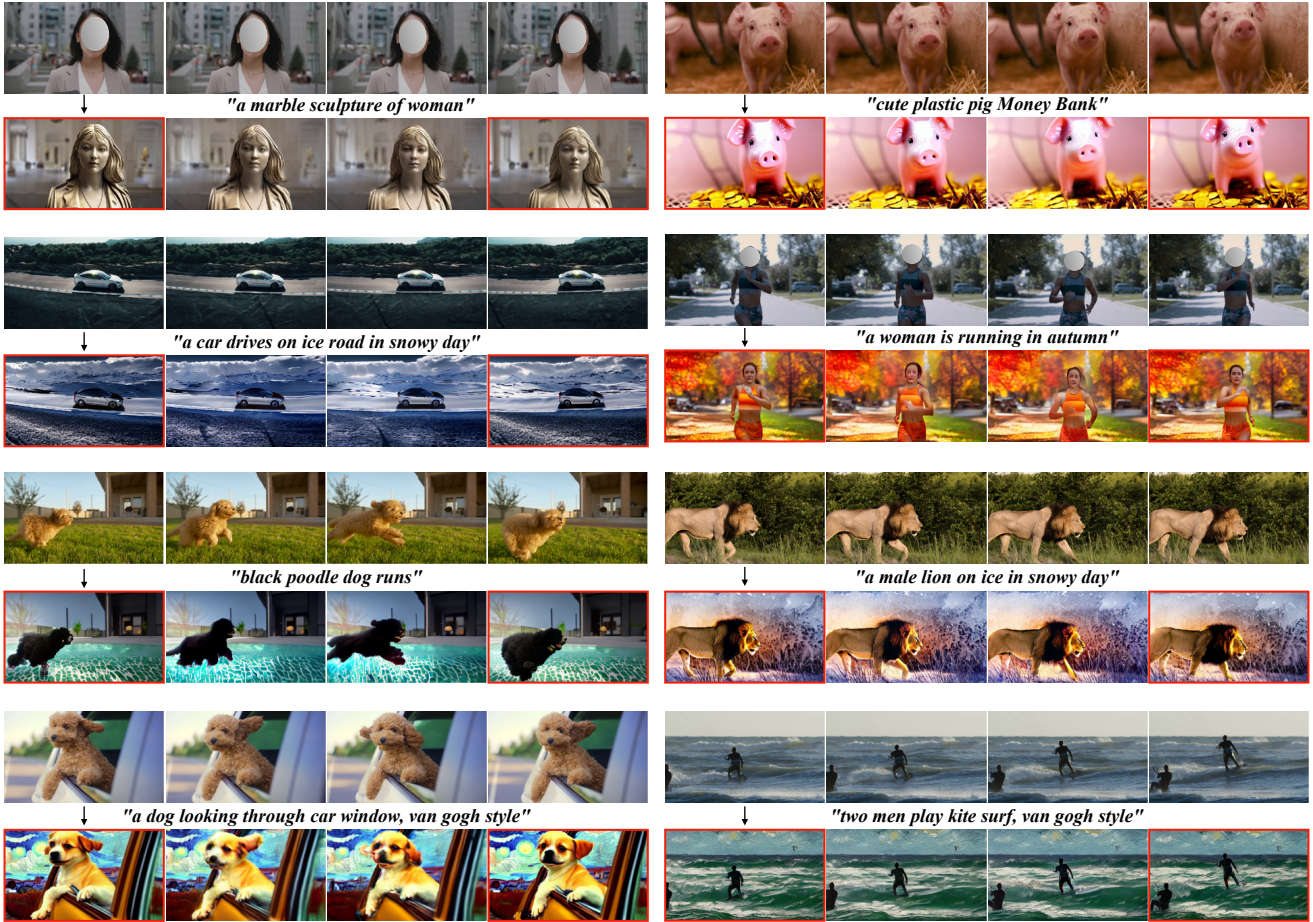


Figure 3. Examples of video editing with MaskINT. Frames with red bounding box are jointly edited keyframes.

Method	DAVIS		ShutterStock		Time
	T.C.	P.C.	T.C.	P.C.	
ControlNet per frame [52]	0.9137	0.3136	0.9419	0.3040	50s
Text2Video-zero [25]	0.9642	0.3124	0.9811	0.3036	60s
TokenFlow [15]	0.9774	0.3169	0.9869	0.3133	150s
ControlVideo-edge [53]	0.9746	0.3143	0.9864	0.3032	120s
MaskINT (ours)	0.9519	0.3112	0.9714	0.3038	22s

Table 1. Quantitative comparisons on the quality of the generated videos. ‘‘T.C.’’ stands for ‘‘temporal consistency’’, and ‘‘P.C.’’ stands for ‘‘prompt consistency’’.

Quantitative Comparisons. Table 1 summarize the performance of these methods on both DAVIS and ShutterStock datasets. Notably, our method achieves comparable performance with diffusion methods, in terms of both temporal consistency and prompt consistency, while brings a significant acceleration in processing speed. In detail, MaskINT is almost 5.5 times faster than ControlVideo [53], whose fully cross-frame attention is computationally extensive. Moreover, MaskINT is nearly 7 times faster than To-

kenFlow [15], whose DDIM inversion is time-consuming. On the contrary, our acceleration is derived from a combination of a lightweight network design and a reduced number of decoding steps in masked generative transformers.

Qualitative Comparisons. Fig. 1 and Fig. 3 show several samples of edited videos with MaskINT. Our method is capable of generating temporally consistent videos that adhere to the provided text prompts. This extends to a wide range of applications with text prompts, encompassing tasks such as stylization, background editing, foreground editing, and more. It also works well on challenging videos with substantial motion, such as jumping and running. Moreover, Fig. 4 provides a qualitative comparison of MaskINT to other baselines. Remarkably, diffusion methods [15, 25, 53] can ensure the consistency of overall appearance, but sometimes cannot maintain the consistency of detailed regions. For example, both TokenFlow [15] and Text2Video-Zero[25] exhibit noticeable artifacts in the leg region of the human subjects. ControlVideo [53] produces

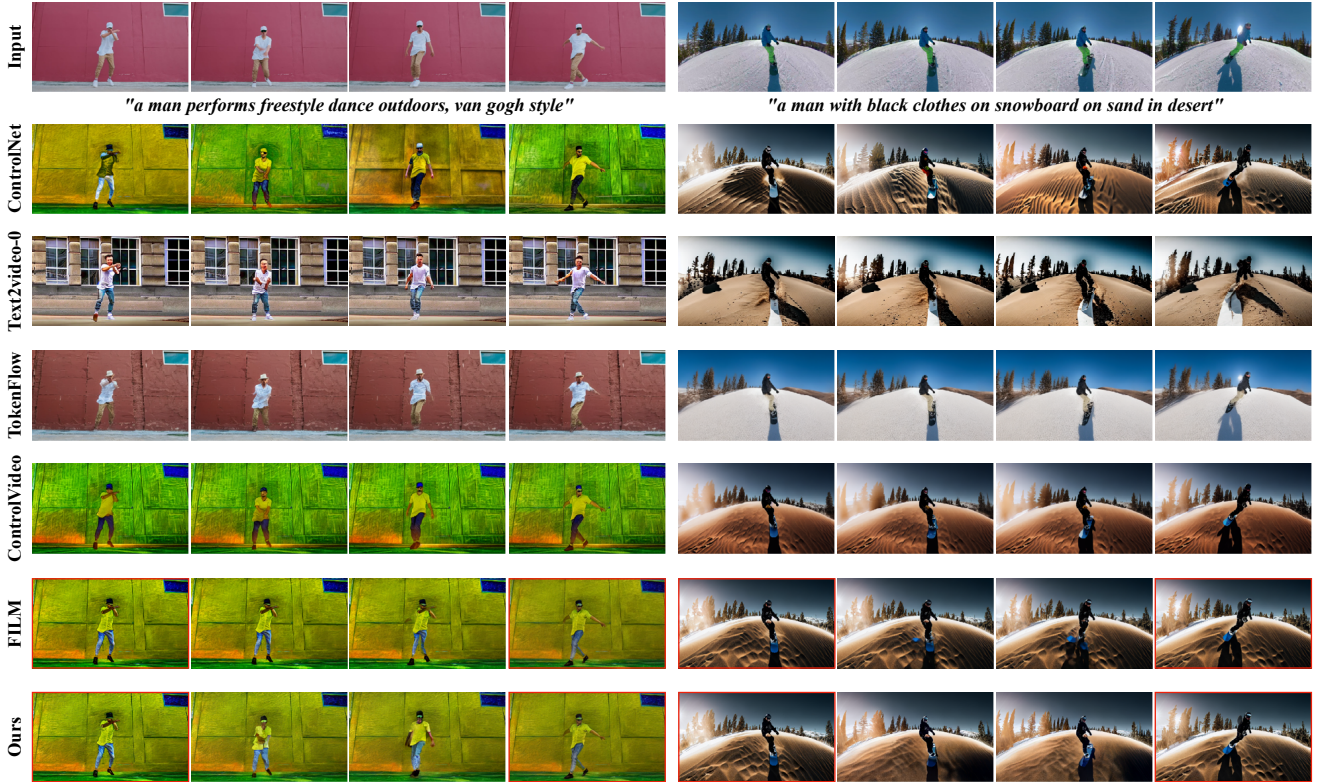


Figure 4. Qualitative comparisons with diffusion-based methods. More examples are shown in Supplementary.

inconsistent hats. The potential explanation lies in the fact that these methods offer control over temporal consistency implicitly. Furthermore, FILM [36] produces videos that deviate from the original motions with the same edited keyframes. Our MaskINT consistently interpolates the intermediate frames based on the structure condition and even maintain better consistency in local regions.

Extension on Long Video Editing. Since the non-autoregressive pipeline generates all video frames simultaneously, it’s challenging for it to edit an entire long video due to GPU memory limitation. Nevertheless, our framework can still be extended to generate long videos by dividing the long video into short clips and progressively performing frame interpolation within each clip. For instance, given a video with 60 frames, we select the 1st, 16th, 31st, 46th, and 60th frames as keyframes. We jointly edit these selected 5 frames together and then perform structure-aware frame interpolation within each pair of consecutive keyframes. As shown in Fig. 5, with this design, our method can still generate consistent long videos. Besides, in this proposed extension, the generation of later frames is decoupled from the generated early frames, which differs from the autoregressive long-video generation pipeline in Phenaki [45]. Consequently, even if some early frames en-

counter difficulties, the generation of later frames can still proceed successfully.



Figure 5. Examples of long video generation. The number indicates the index of frame. More examples are in Supplementary.

5.3. Ablation Studies

Video Frame Interpolations We conduct a quantitative evaluation on the performance of our structure-aware interpolation module. In this ablation study, we perform frame interpolation using the original keyframes to reconstruct the original intermediate frames, and compare the interpolated frames with the original video frames at the

pixel level. We use same testing samples from DAVIS and Shutterstock datasets, employing peak signal-to-noise ratio (PSNR), learned perceptual image patch similarity (LPIPS), and structured similarity (SSIM) as the evaluation metrics. We benchmark our method against two state-of-the-art VFI methods, namely FILM [36] and RIFE [22]. We also show-case the performance of applying VQ-GAN [12] to all video frames, serving as an upper bound for our method.

As in Table 2, our method significantly outperforms VFI methods on all evaluation metrics, with the benefit of the structure guidance from the intermediate frames. Furthermore, Fig. 6 shows qualitative comparison between video frame interpolation methods FILM [36] and MaskINT. Even when confronted with significant motion between two frames, our approach successfully reconstructs the original video, maintaining consistent motion through the aid of structural guidance. In contrast, FILM introduces undesirable artifacts, including distorted background, duplicated cat hands, and the absence of a camel’s head, etc. The major reason is that current VFI models mainly focus on generating slow-motion effects and enhancing frame rate, making them less effective in handling frames with large motions, which usually requires a better semantic understanding. Additionally, the absence of structural guidance poses a challenge for these VFI methods in accurately aligning generated videos with the original motion.

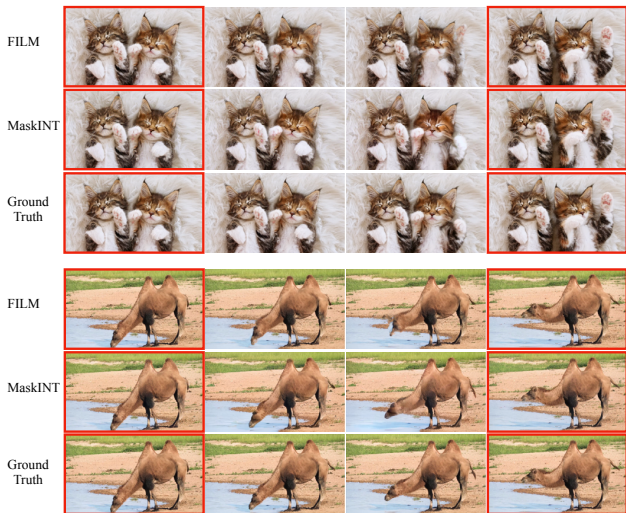


Figure 6. Qualitative comparisons on video reconstruction with original RGB frames. Frames with red bounding box are given.

Number of of keyframes Although our model is trained with frame interpolation by default, MaskINT can seamlessly generalize to an arbitrary number of keyframes without finetuning. We assess the impact of varying the quantity of keyframes on the generation performance. As shown in the left part of Table 3, with an increase in the number

Method	DAVIS			ShutterStock		
	PSNR↑	SSIM↑	LPIPS↓	PSNR↑	SSIM↑	LPIPS↓
RIFE [22]	17.31	0.5195	0.2512	20.44	0.7210	0.1533
FILM [36]	17.00	0.5011	0.2363	20.90	0.7453	0.1246
MaskINT	22.15	0.6332	0.1483	24.19	0.7616	0.1097
VQGAN (ground truth)	25.66	0.7429	0.0784	27.81	0.8327	0.0561

Table 2. Quantitative comparisons on video frame interpolation with original keyframes.

of keyframes, the model exhibits an improvement in performance. Generally, with more information, performing frame interpolation is easier. However, simultaneously editing more keyframes requires longer time due to the global attention among them.

Decoding steps We also explore the number of decoding steps of the masked generative transformers in the second stage. The right part of Table 3 shows that more decoding steps can bring slight improvement on the temporal consistency, but requires more time. Considering the trade-off between performance and efficiency, we chose $K = 32$ steps by default in all experiments.

# keyframes	T.C.	P.C.	Time	#decoding step K	T.C.	P.C.	Time
1	0.9690	0.2984	19s	16	0.9691	0.3038	15s
2	0.9714	0.3038	22s	32	0.9714	0.3038	22s
3	0.9721	0.3051	26s	64	0.9719	0.3040	33s
4	0.9728	0.3069	29s	128	0.9720	0.3041	62s
6	0.9737	0.3035	35s				

Table 3. Ablation study on Shutterstock dataset of the number of keyframes and the number of decoding steps K . “T.C.” stands for “temporal consistency” and “P.C.” stands for “prompt consistency”.

6. Limitation and Future Work

One potential limitation of our approach is that it still necessitates the use of diffusion-based methods for keyframe editing in the initial stage, which can still be somewhat time-consuming. As for the future work, given that our approach disentangles video editing into two distinct stages, we intend to explore the integration of token-based methods, like Muse [8], for image editing. This endeavor aims to further enhance the efficiency of the initial stage.

7. Conclusion

We propose MaskINT towards consistent and efficient video editing with text prompt. MaskINT disentangle this task into keyframes joint editing with diffusion methods and structure-aware frame interpolation with non-autoregressive masked transformers. Experimental results demonstrate that MaskINT achieves comparable performance with pure diffusion-based methods while significantly reduces the inference time. Moreover, our work demonstrates the substantial promise of non-autoregressive generative transformers within the realm of video editing.

References

- [1] Dina Bashkirova, José Lezama, Kihyuk Sohn, Kate Saenko, and Irfan Essa. Masksketch: Unpaired structure-guided masked image generation. In *CVPR*, pages 1879–1889, 2023. 2
- [2] Gedas Bertasius, Heng Wang, and Lorenzo Torresani. Is space-time attention all you need for video understanding? In *ICML*, 2021. 4
- [3] Andreas Blattmann, Robin Rombach, Huan Ling, Tim Dockhorn, Seung Wook Kim, Sanja Fidler, and Karsten Kreis. Align your latents: High-resolution video synthesis with latent diffusion models. In *CVPR*, pages 22563–22575, 2023. 1
- [4] Tim Brooks, Aleksander Holynski, and Alexei A Efros. Instructpix2pix: Learning to follow image editing instructions. In *CVPR*, pages 18392–18402, 2023. 1, 3
- [5] Tom Brown, Benjamin Mann, Nick Ryder, Melanie Subbiah, Jared D Kaplan, Prafulla Dhariwal, Arvind Neelakantan, Pranav Shyam, Girish Sastry, Amanda Askell, et al. Language models are few-shot learners. *NeurIPS*, 33:1877–1901, 2020. 2
- [6] Duygu Ceylan, Chun-Hao P Huang, and Niloy J Mitra. Pix2video: Video editing using image diffusion. In *ICCV*, pages 23206–23217, 2023. 3
- [7] Huiwen Chang, Han Zhang, Lu Jiang, Ce Liu, and William T Freeman. Maskgit: Masked generative image transformer. In *CVPR*, pages 11315–11325, 2022. 1, 2, 3, 4, 5
- [8] Huiwen Chang, Han Zhang, Jarred Barber, AJ Maschinot, Jose Lezama, Lu Jiang, Ming-Hsuan Yang, Kevin Murphy, William T Freeman, Michael Rubinstein, et al. Muse: Text-to-image generation via masked generative transformers. *ICML*, 2023. 1, 2, 8
- [9] Guillaume Couairon, Jakob Verbeek, Holger Schwenk, and Matthieu Cord. Diffedit: Diffusion-based semantic image editing with mask guidance. *arXiv preprint arXiv:2210.11427*, 2022. 3
- [10] Jacob Devlin, Ming-Wei Chang, Kenton Lee, and Kristina Toutanova. Bert: Pre-training of deep bidirectional transformers for language understanding. *NAACL*, 2019. 1, 3
- [11] Abhimanyu Dubey, Filip Radenovic, Dhruv Mahajan, and Vignesh Ramanathan. Retina vq. 2023. 5
- [12] Patrick Esser, Robin Rombach, and Bjorn Ommer. Taming transformers for high-resolution image synthesis. In *CVPR*, pages 12873–12883, 2021. 1, 2, 3, 4, 8
- [13] Patrick Esser, Johnathan Chiu, Parmida Atighehchian, Jonathan Granskog, and Anastasis Germanidis. Structure and content-guided video synthesis with diffusion models. *ICCV*, 2023. 1, 3
- [14] Songwei Ge, Thomas Hayes, Harry Yang, Xi Yin, Guan Pang, David Jacobs, Jia-Bin Huang, and Devi Parikh. Long video generation with time-agnostic vqgan and time-sensitive transformer. In *ECCV*, pages 102–118. Springer, 2022. 2
- [15] Michal Geyer, Omer Bar-Tal, Shai Bagon, and Tali Dekel. Tokenflow: Consistent diffusion features for consistent video editing. *arXiv preprint arXiv:2307.10373*, 2023. 1, 3, 4, 5, 6
- [16] Agrim Gupta, Stephen Tian, Yunzhi Zhang, Jiajun Wu, Roberto Martín-Martín, and Li Fei-Fei. Maskvit: Masked visual pre-training for video prediction. In *ICLR*, 2023. 1, 2, 4
- [17] Amir Hertz, Ron Mokady, Jay Tenenbaum, Kfir Aberman, Yael Pritch, and Daniel Cohen-Or. Prompt-to-prompt image editing with cross attention control. *arXiv preprint arXiv:2208.01626*, 2022. 3
- [18] Jonathan Ho, Ajay Jain, and Pieter Abbeel. Denoising diffusion probabilistic models. *NeurIPS*, 33:6840–6851, 2020. 1, 3
- [19] Jonathan Ho, William Chan, Chitwan Saharia, Jay Whang, Ruiqi Gao, Alexey Gritsenko, Diederik P Kingma, Ben Poole, Mohammad Norouzi, David J Fleet, et al. Imagen video: High definition video generation with diffusion models. *arXiv preprint arXiv:2210.02303*, 2022. 1, 3
- [20] Wenyi Hong, Ming Ding, Wendi Zheng, Xinghan Liu, and Jie Tang. Cogvideo: Large-scale pretraining for text-to-video generation via transformers. *ICLR*, 2023. 2
- [21] Lianghua Huang, Di Chen, Yu Liu, Yujun Shen, Deli Zhao, and Jingren Zhou. Composer: Creative and controllable image synthesis with composable conditions. *arXiv preprint arXiv:2302.09778*, 2023. 3
- [22] Zhewei Huang, Tianyuan Zhang, Wen Heng, Boxin Shi, and Shuchang Zhou. Real-time intermediate flow estimation for video frame interpolation. In *ECCV*, pages 624–642. Springer, 2022. 3, 8
- [23] Huaizu Jiang, Deqing Sun, Varun Jampani, Ming-Hsuan Yang, Erik Learned-Miller, and Jan Kautz. Super slo-mo: High quality estimation of multiple intermediate frames for video interpolation. In *CVPR*, pages 9000–9008, 2018. 3
- [24] Bahjat Kawar, Shiran Zada, Oran Lang, Omer Tov, Huiwen Chang, Tali Dekel, Inbar Mosseri, and Michal Irani. Imagic: Text-based real image editing with diffusion models. In *CVPR*, pages 6007–6017, 2023. 3
- [25] Levon Khachatryan, Andranik Movsisyan, Vahram Tadevosyan, Roberto Henschel, Zhangyang Wang, Shant Navasardyan, and Humphrey Shi. Text2video-zero: Text-to-image diffusion models are zero-shot video generators. *ICCV*, 2023. 1, 3, 5, 6
- [26] Guillaume Le Moing, Jean Ponce, and Cordelia Schmid. Ccvs: context-aware controllable video synthesis. *NeurIPS*, 34:14042–14055, 2021. 2
- [27] Ilya Loshchilov and Frank Hutter. Decoupled weight decay regularization. In *ICLR*, 2019. 5
- [28] Liying Lu, Ruizheng Wu, Huajia Lin, Jiangbo Lu, and Jiaya Jia. Video frame interpolation with transformer. In *CVPR*, pages 3532–3542, 2022. 3
- [29] Chenlin Meng, Yutong He, Yang Song, Jiaming Song, Jiajun Wu, Jun-Yan Zhu, and Stefano Ermon. Sdedit: Guided image synthesis and editing with stochastic differential equations. *ICLR*, 2022. 3
- [30] Chong Mou, Xintao Wang, Liangbin Xie, Jian Zhang, Zhongqiang Qi, Ying Shan, and Xiaohu Qie. T2i-adapter: Learning adapters to dig out more controllable ability for text-to-image diffusion models. *arXiv preprint arXiv:2302.08453*, 2023. 3

- [31] Simon Niklaus, Long Mai, and Feng Liu. Video frame interpolation via adaptive separable convolution. In *ICCV*, pages 261–270, 2017. 3
- [32] Gaurav Parmar, Krishna Kumar Singh, Richard Zhang, Yijun Li, Jingwan Lu, and Jun-Yan Zhu. Zero-shot image-to-image translation. In *ACM SIGGRAPH 2023 Conference Proceedings*, pages 1–11, 2023. 3
- [33] Jordi Pont-Tuset, Federico Perazzi, Sergi Caelles, Pablo Arbeláez, Alexander Sorkine-Hornung, and Luc Van Gool. The 2017 davis challenge on video object segmentation. *arXiv:1704.00675*, 2017. 5
- [34] Chenyang Qi, Xiaodong Cun, Yong Zhang, Chenyang Lei, Xintao Wang, Ying Shan, and Qifeng Chen. Fatezero: Fusing attentions for zero-shot text-based video editing. *ICCV*, 2023. 1, 3, 5
- [35] Alec Radford, Jong Wook Kim, Chris Hallacy, Aditya Ramesh, Gabriel Goh, Sandhini Agarwal, Girish Sastry, Amanda Askell, Pamela Mishkin, Jack Clark, et al. Learning transferable visual models from natural language supervision. In *ICML*, pages 8748–8763, 2021. 5
- [36] Fitsum Reda, Janne Kontkanen, Eric Tabellion, Deqing Sun, Caroline Pantofaru, and Brian Curless. Film: Frame interpolation for large motion. In *ECCV*, 2022. 3, 5, 7, 8
- [37] Robin Rombach, Andreas Blattmann, Dominik Lorenz, Patrick Esser, and Björn Ommer. High-resolution image synthesis with latent diffusion models. In *CVPR*, pages 10684–10695, 2022. 1, 2, 3
- [38] Chitwan Saharia, William Chan, Saurabh Saxena, Lala Li, Jay Whang, Emily L Denton, Kamyar Ghasemipour, Raphael Gontijo Lopes, Burcu Karagol Ayan, Tim Salimans, et al. Photorealistic text-to-image diffusion models with deep language understanding. *NeurIPS*, 35:36479–36494, 2022. 1
- [39] Hyeonjun Sim, Jihyong Oh, and Munchurl Kim. Xvfi: extreme video frame interpolation. In *ICCV*, pages 14489–14498, 2021. 3
- [40] Uriel Singer, Adam Polyak, Thomas Hayes, Xi Yin, Jie An, Songyang Zhang, Qiyuan Hu, Harry Yang, Oron Ashual, Oran Gafni, et al. Make-a-video: Text-to-video generation without text-video data. *ICLR*, 2023. 1, 3
- [41] Kihyuk Sohn, Nataniel Ruiz, Kimin Lee, Daniel Castro Chin, Irina Blok, Huiwen Chang, Jarred Barber, Lu Jiang, Glenn Entis, Yuanzhen Li, et al. Styledrop: Text-to-image generation in any style. *arXiv preprint arXiv:2306.00983*, 2023. 2
- [42] Jiaming Song, Chenlin Meng, and Stefano Ermon. Denoising diffusion implicit models. *ICLR*, 2021. 3
- [43] Narek Tumanyan, Michal Geyer, Shai Bagon, and Tali Dekel. Plug-and-play diffusion features for text-driven image-to-image translation. In *CVPR*, pages 1921–1930, 2023. 1, 3
- [44] Ashish Vaswani, Noam Shazeer, Niki Parmar, Jakob Uszkoreit, Llion Jones, Aidan N Gomez, Łukasz Kaiser, and Illia Polosukhin. Attention is all you need. *NeurIPS*, 30, 2017. 1, 3, 4
- [45] Ruben Villegas, Mohammad Babaeizadeh, Pieter-Jan Kindermans, Hernan Moraldo, Han Zhang, Mohammad Taghi Saffar, Santiago Castro, Julius Kunze, and Dumitru Erhan. Phenaki: Variable length video generation from open domain textual descriptions. In *ICLR*, 2023. 2, 7
- [46] Xiang Wang, Hangjie Yuan, Shiwei Zhang, Dayou Chen, Jiuniu Wang, Yingya Zhang, Yujun Shen, Deli Zhao, and Jingren Zhou. Videocomposer: Compositional video synthesis with motion controllability. *arXiv preprint arXiv:2306.02018*, 2023. 3
- [47] Jay Zhangjie Wu, Yixiao Ge, Xintao Wang, Weixian Lei, Yuchao Gu, Wynne Hsu, Ying Shan, Xiaohu Qie, and Mike Zheng Shou. Tune-a-video: One-shot tuning of image diffusion models for text-to-video generation. *ICCV*, 2023. 3, 4, 5
- [48] Saining Xie and Zhuowen Tu. Holistically-nested edge detection. In *ICCV*, pages 1395–1403, 2015. 4
- [49] Shuai Yang, Yifan Zhou, Ziwei Liu, and Chen Change Loy. Rerender a video: Zero-shot text-guided video-to-video translation. *ACM SIGGRAPH Asia Conference Proceedings*, 2023. 3
- [50] Jiahui Yu, Xin Li, Jing Yu Koh, Han Zhang, Ruoming Pang, James Qin, Alexander Ku, Yuanzhong Xu, Jason Baldridge, and Yonghui Wu. Vector-quantized image modeling with improved VQGAN. In *ICLR*, 2022. 2
- [51] Lijun Yu, Yong Cheng, Kihyuk Sohn, José Lezama, Han Zhang, Huiwen Chang, Alexander G Hauptmann, Ming-Hsuan Yang, Yuan Hao, Irfan Essa, et al. Magvit: Masked generative video transformer. In *CVPR*, pages 10459–10469, 2023. 1, 2, 4
- [52] Lvmin Zhang and Maneesh Agrawala. Adding conditional control to text-to-image diffusion models. *ICCV*, 2023. 1, 3, 4, 6
- [53] Yabo Zhang, Yuxiang Wei, Dongsheng Jiang, Xiaopeng Zhang, Wangmeng Zuo, and Qi Tian. Controlvideo: Training-free controllable text-to-video generation. *arXiv preprint arXiv:2305.13077*, 2023. 1, 3, 4, 5, 6
- [54] Zhixing Zhang, Ligong Han, Arnab Ghosh, Dimitris N Metaxas, and Jian Ren. Sine: Single image editing with text-to-image diffusion models. In *CVPR*, pages 6027–6037, 2023. 3

MaskINT: Video Editing via Interpolative Non-autoregressive Masked Transformers

Supplementary Material

8. Diverse Structural Conditions

Although we by default utilize HED edge map as our structure condition for both stages, our method can also employ other structural controls in both stages due to the disentanglement. In this study, we explore utilizing ControlNet with depth map to perform key frame editing, and using the depth map as the guidance to perform structure-aware frame interpolation. Additionally, we explore various combinations of these approaches. As summarized in Table 4, all of these combinations achieve the same level of performance. The performance of prompt consistency (P.C.) is determined by the specific key frame editing methods employed. For the second stage, depth control typically offers greater flexibility than HED edge control for frame interpolation. This could be the potential reason for the slightly worse performance in temporal consistency with edge-based key frame editing.

Stage1	Stage2	T.C.	P.C
HED edge	HED edge	0.9714	0.3038
depth map	HED edge	0.9713	0.3159
HED edge	depth map	0.9683	0.3035
depth map	depth map	0.9719	0.3171

Table 4. Quantitative comparisons of the combination of varied structural conditions in each stage on Shutterstock. “T.C.” stands for “temporal consistency”, and “P.C.” stands for “prompt consistency”.

9. Additional Examples for Comparisons

We add more comparisons with diffusion methods in Fig. 8. Our methods can maintain the temporal consistency among variant examples like other pure-diffusion methods.

10. Additional Editing Examples

We present more video editing examples in Figure 9 to show the generalization of our method.

11. Example of Failure Cases

Since we disentangle the video editing tasks into two separate stage, the final performance of the generated video depends on the key frame editing in the first stage. In certain challenging scenarios, the attention-based key frame editing stage struggles to produce consistent frames, primarily

due to the complexity of the scene or the presence of exceptionally large motion. In this case, our MaskINT can still interpolate the intermediate frames, albeit with the potential for introducing artifacts. Figure 7 show some failure cases when the first stage fails.

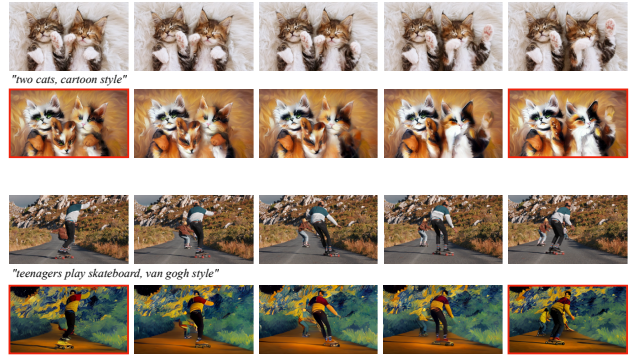


Figure 7. Examples of failure cases.

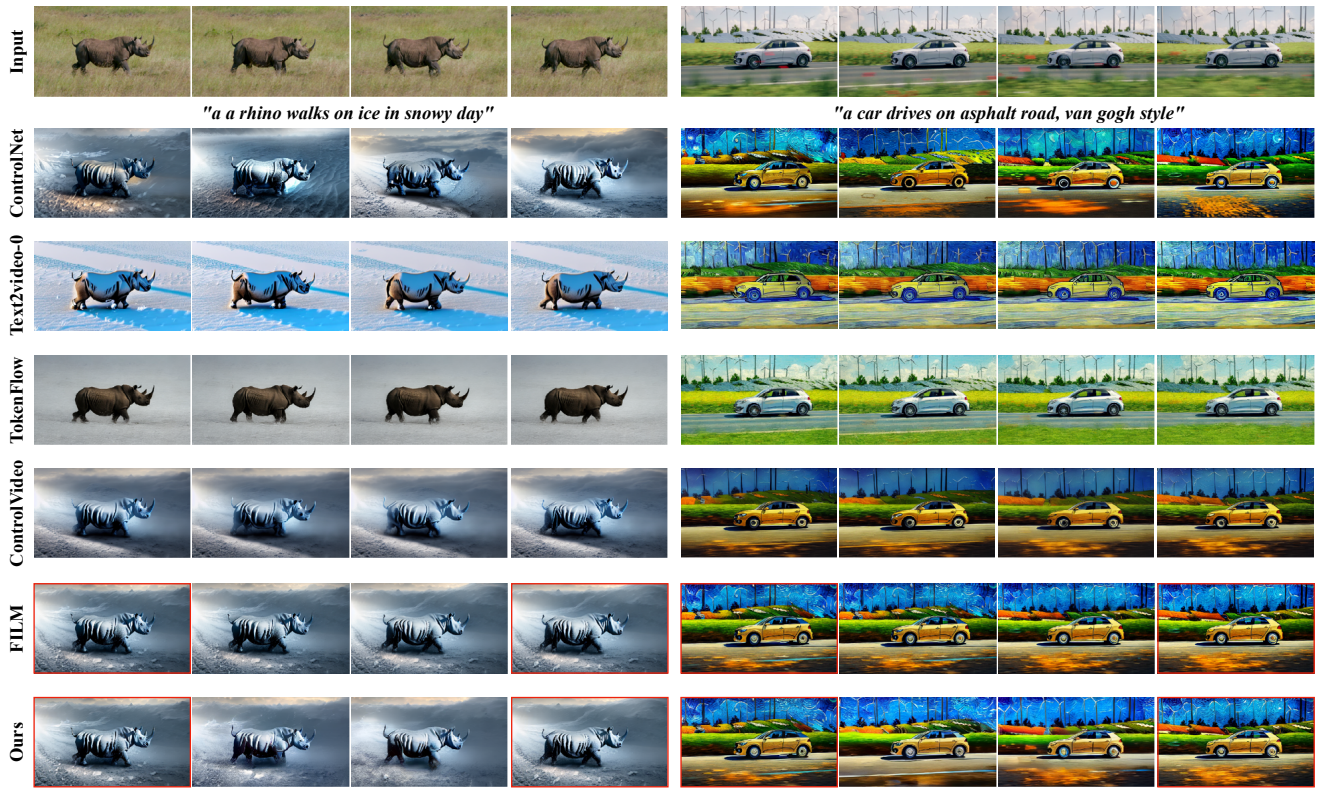


Figure 8. Additional Qualitative comparisons with diffusion-based methods. Frames with red bounding box are jointly edited keyframes.

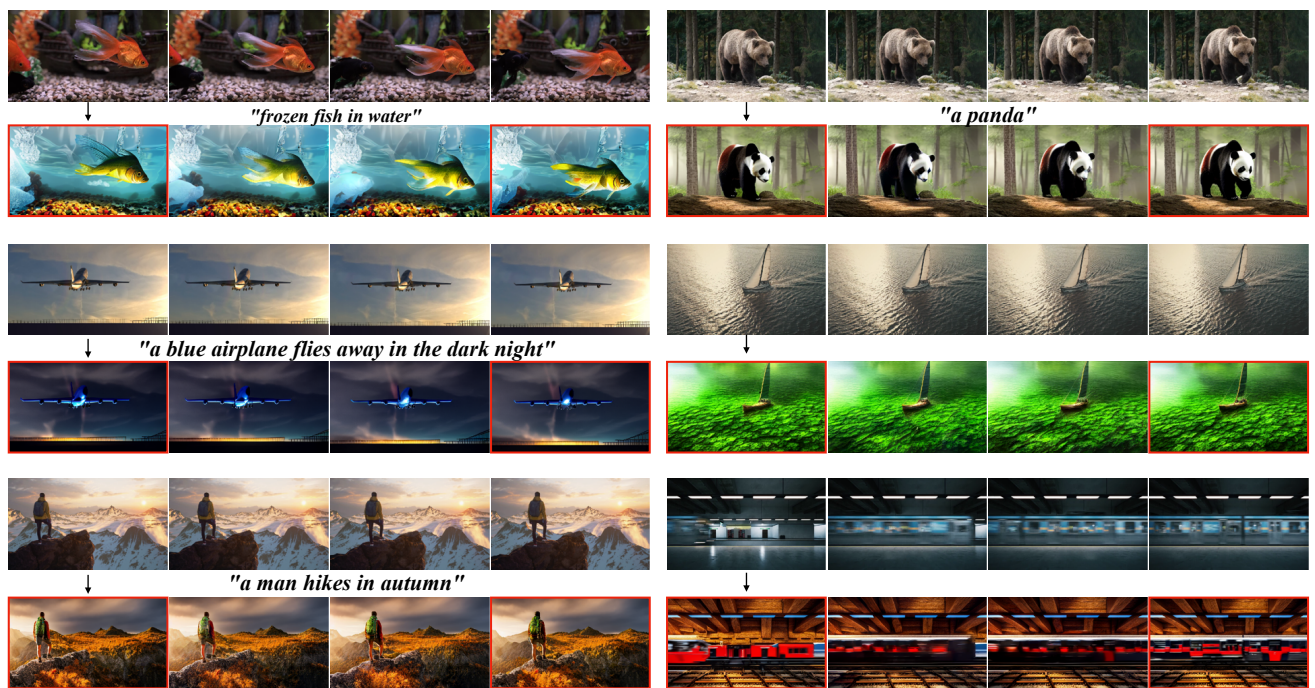


Figure 9. Additional Editing examples with MaskINT. Frames with red bounding box are jointly edited keyframes.